Carbon-based materials: From fullerene nanostructures to functionalized carbon nanotubes*

Nikos Tagmatarchis and Maurizio Prato‡

Consorzio INSTM, UdR di Trieste, Dipartimento di Scienze Farmaceutiche, Università di Trieste, Piazzale Europa 1, Trieste 34127, Italy

Abstract: Self-assembly in morphological organization of various fullerene derivatives affords different supramolecular architectures. Nanospheres, tubules, and bundles of nanorods are formed depending on the nature of the organic group in the fullerene unit. The current work highlights an efficient method to fabricate almost perfect and uniformly shaped nanocrystals in a novel connection between spherical fullerene-based materials and fibrous nanotubes. In a parallel research line, carbon nanotubes (CNTs) have been functionalized using 1,3-dipolar cycloaddition of azomethine ylides. The organically functionalized CNTs, having improved solubility and potential for applications, are characterized by standard analytical methods as well as microscopy techniques.

Keywords: Fullerenes; carbon nanotubes; self-assembly; nanostructures; nanotechnology; cycloadditions.

INTRODUCTION

The spontaneous association of molecules into structurally well-defined aggregates formed by non-covalent bonds through self-assembly processes has the potential of generating structures in the nanometer scale which are currently inaccessible via rational chemical synthesis [1]. Nowadays, developing techniques for synthesizing and characterizing nanostructured assemblies is one of the great challenges facing chemistry and materials science. In order for the final assembly to be stable enough and to have well-defined shapes, the noncovalent interactions between individual molecules must be stable and strong. Thus, to achieve acceptable stability, molecules in self-assembled aggregates should be joined by a high number of weak noncovalent interactions. Moreover, these interactions must be more favorable energetically than the competing interactions with the solvent and must be able to overwhelm the entropic advantages of disintegration of the ordered aggregate into disordered or dissociated states.

The ability to fabricate distinct one-, two-, or three-dimensional supramolecular patterns, potentially exploitable for bottom-up construction of molecular-based devices, demands the development of general and reliable approaches to control the aggregation processes. Recently, different techniques for synthesizing and characterizing nanostructured assemblies have been developed at the interface between chemistry and materials science [2–10].

Herein we show how the hydrophobic all-carbon fullerene sphere combined with hydrophilic oligoethylene glycol ammonium salt chains assembles in either tubules, bundles of wires, or spheres,

and how the fullerene derivatives are connected to the fibrous carbon nanotubes (CNTs) and their soluble derivatives.

FULLERENE NANOSTRUCTURES

C_{60} is the most abundant, least expensive, and, therefore, most thoroughly studied member of the all-carbon hollow-cluster materials, namely, fullerenes. The covalent functionalization chemistry of C_{60} has developed dramatically during the last decade: a wide variety of synthetic protocols, successfully applied to C_{60}, have established this novel form of carbon as a useful building block in organic synthesis. The main advantage gained upon modification of fullerenes is a substantial increase in their solubility, in addition to the presence of new functionalities. The difficult processibility of intact fullerenes in most organic solvents is overcome with the aid of functionalization, and, thus, fullerenes are placed in pole position in the run for innovative technological applications. The existence of a great diversity of synthetic protocols combined with the plethora of chemical reactions that have been applied to C_{60} has brought about the formation of a huge number of functionalized fullerenes. Fundamentally, it is the combination of the unique structural, physicochemical, and electronic properties of the fullerenes with the special characteristics of the added groups that eventually leads to the development of new materials with enormous potential in fascinating and widespread technological and biological applications. However, while the covalent functionalization of C_{60} has met such rapid development, supramolecular fullerene chemistry has not been explored to such an extent.

The 1,3-dipolar cycloaddition of azomethine ylides has been widely utilized as a synthetic procedure for the synthesis of modified fullerenes [11–14]. Azomethine ylides are reactive intermediates generated in situ by many different ways. Most popular approaches encompass: (i) decarboxylation of immonium salts derived from thermal condensation of α-amino acids and aldehydes (alternatively ketones); (ii) thermal ring-opening of aziridines. Thus, when azomethine ylides are added to C_{60}, fulleropyrrolidines are formed, in which a pyrrolidine ring is fused to a junction between two six-membered rings of a fullerene sphere (Scheme 1).
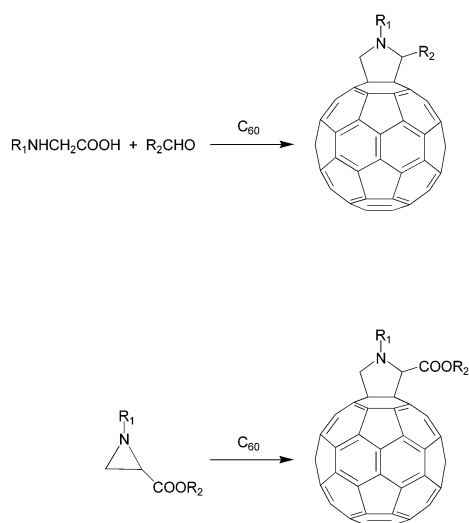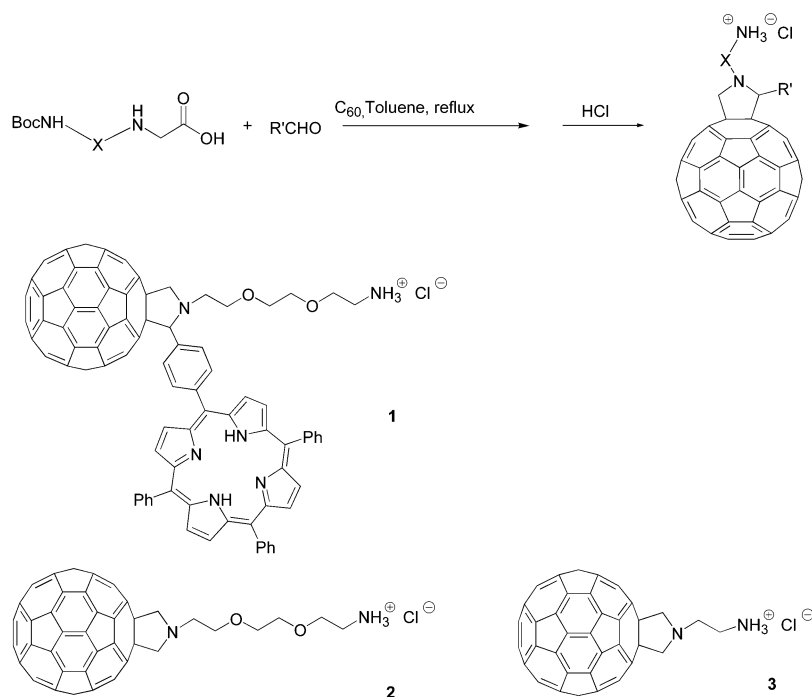

Scheme 1

The key features of this type of reaction are summarized in the following: (i) utilization of functionalized aldehydes leads to the formation of 2-substituted fulleropyrrolidines whereas utilization of N-substituted glycines affords N-substituted fulleropyrrolidines and (ii) by controlling the stoichiome-

try of the reagents and the reaction conditions, mono-fulleropyrrolidines as main products are formed. Structurally different derivatives can be obtained by either using properly functionalized azomethine ylides or by modifying a fulleropyrrolidine intermediate. Thus, a wide variety of compounds specifically designed for diverse applications have been realized.

The key components of this work are a porphyrin macrocycle, the C_{60} cage, and oligoethylene glycol/ammonium salt chains. The porphyrin moiety was selected for its electron donor properties, C_{60} was chosen for its electron-accepting capacity so that their combination holds promise for technological applications such as photovoltaic devices and plastic solar cells [15–19], while the oligoethylene glycol/ammonium salt chain was introduced for water solubility. The photoinduced electron-transfer process in fullerene–porphyrin hybrid systems can be controlled by covalently linking donor and acceptor moieties incorporating fullerene units. In addition, it has already been shown that the rates of forward and back electron transfer in such hybrid systems strongly depend on the molecular topology [20–23]. In other words, the extent and the rate of charge recombination could be decreased by modulating the separation (or the spatial orientation) of the donor and acceptor units while maintaining a high rate of charge separation.

The compounds used in this work, synthesized by 1,3-dipolar cycloaddition of azomethine ylides to C_{60}, are shown in Scheme 2. The combination of the hydrophobic fullerene core with the hydrophilic oligoethylene glycol ammonium salt groups and/or the porphyrin skeleton forces these compounds to assemble differently when dissolved in aqueous media.

Scheme 2

Briefly describing the experimental procedure, various types of aggregates were morphologically organized by ultrasonication of water dispersions of the examined fulleropyrrolidine materials **1**, **2**, and **3**. After centrifugation of the heterogeneous mixture, a drop from the clear supernatant solution was transferred onto a copper grid (3.0 mm 200 mesh), coated with formvar film for transmission electron microscopy (TEM) study. Afterward, air-drying images were taken on a Philips TEM 208 at an accelerating voltage of 100 kV.

The noncovalent $\pi-\pi$ stacking interactions between porphyrin units and hydrophobic interactions between C_{60} molecules as well as the interactions between porphyrin-C_{60} are the driving force for self-assembling. Thus, tubular superstructures reaching 30 nm in diameter and 500 nm in length were formed when compound **1** was sonicated in water and visualized with the aid of TEM as shown in Fig. 1.
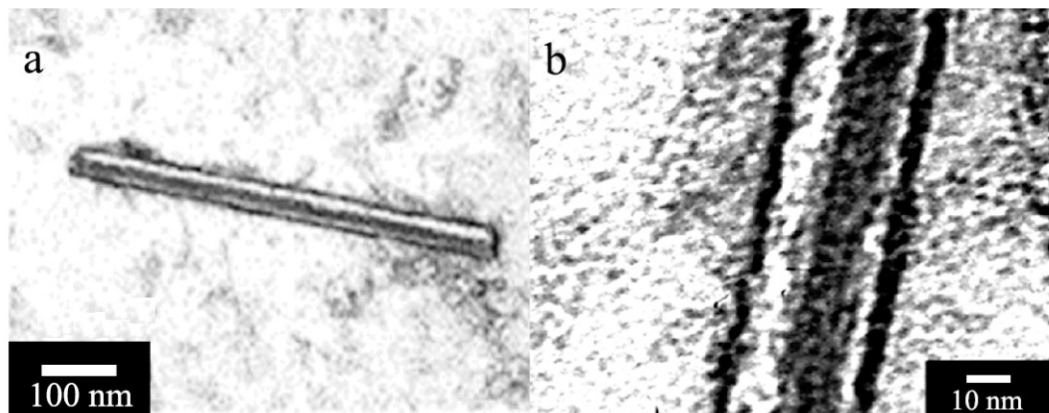

Fig. 1 TEM micrographs of the structures generated by self-assembly of compound **1**.

On the other hand, compound **2**, which can be conceptually derived from **1** by removing the porphyrin fragment, organizes in water differently. Thus, bundles of wires of 4 nm in diameter and several microns length are detected for compound **2** by TEM as shown in Fig. 2a. Furthermore, changing the oligoethylene glycol chain to a short aliphatic one in fulleropyrrolidine **3**, results in another morphologically organized arrangement. Thus, superstructures of nanospheres with diameters ranging from 500 nm to 1.2 μm aggregate together as shown in Fig. 2b.
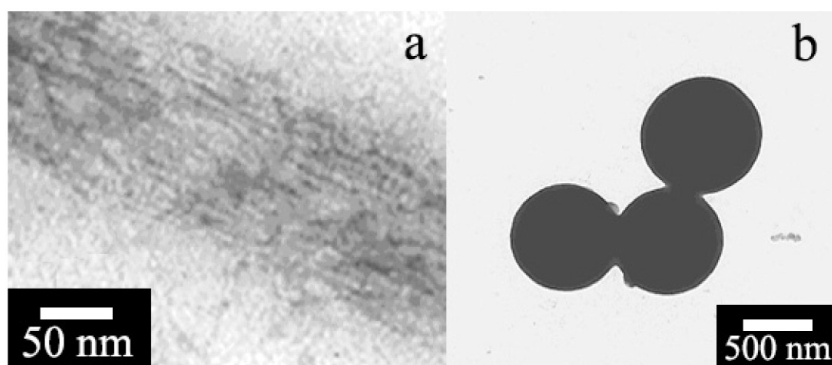

Fig. 2 TEM micrographs of the forms generated by self-assembly of compounds **2** (a) and **3** (b).

The driving force for the formation of each superstructure is the result of a subtle balance between hydrophobic interactions and specific, directional interactions between the molecules. The examined compounds are all amphiphilic, but with different water solubilities. The least water-soluble compound **3** aggregates in spheres, therefore suggesting that the driving force for aggregation is hydrophobic and nondirectional. However, formation of infinite long-rod superstructures, as in the case of compound **2**, indicates a lesser role played by hydrophobicity. The resulting superstructures can still occur without the presence of preferred or directional interactions. Eventually, the presence of directionality is posi-

tively introduced in compound **1** by the porphyrin unit and causes the finite length of the nanotubules and their more regular structures.

The self-organization of fullerene-based materials from spherically shaped (e.g., compound **3**) to fibrous-structurally materials (e.g., compound **1**) shows that indeed the morphology of supramolecular aggregates in the nanometer level can be tuned in a fine way [24–26]. In such a way of aggregation, fullerenes are perfectly morphologically connected to CNTs via self-assembly—an astonishing process that up to now cannot be performed by any rational modification of fullerene-based materials.

CARBON NANOTUBES

As effectively long, thin cylinders of graphite, CNTs seem to be ideal building blocks in nanotechnology. The almost perfect one-dimensional character of CNTs coupled with unique and outstanding physical and electronic properties render them ideal components for the development of novel nanoscale devices. Extraordinary properties have been attributed to CNTs, so that a range of technological applications have been envisaged, ranging from wiring in integrated circuits and nanoscale components to composite materials with improved functional characteristics. Advances in production processes have resulted in obtaining CNTs with high structural perfection: relatively large amounts can now be produced of either single-walled carbon nanotubes (SWNTs) consisting of a single graphite sheet seamlessly wrapped into a cylindrical tube with diameter of 0.4–3 nm, or multi-walled carbon nanotubes (MWNTs) which comprise an array of concentric cylinders with diameter of 1.4–100 nm, respectively. Furthermore, depending on the chirality of their atomic structure, CNTs can be metals or semiconductors with a band gap that is inversely proportional to their diameter.

Due to π–π interactions, CNTs aggregate strongly in bundles similarly to the cohesion between layers of pure graphite. In addition, according to their size, CNTs behave as large macromolecules, making their manipulation, characterization, and analytical investigation very difficult. Therefore, to fulfill expectations, manipulation and processing of CNTs in organic solvents is crucial. The study of chemical modification of CNTs at a molecular level is still in its infancy mainly due to their high insolubility in organic solvents. Derivatization through organic functionalization is, therefore, desirable as it improves both solubility and processibility, with the opportunity for fabricating novel nanostructures [27–35]. Consequently, the compatibility of CNTs with other materials, such as polymers, should be strongly improved. In principle, once properly functionalized CNTs become soluble, their solution properties can be studied.

Considerable efforts have been devoted to the functionalization of CNTs that aids debundling and improve CNT solubility [36–42]. Inspired from the 1,3-dipolar cycloaddition of azomethine ylides to fullerenes, we have succeeded in functionalizing and thus solubilizing CNTs [43–52]. Briefly, CNTs were suspended in dimethyl formamide (DMF), an excess of aldehyde and α-amino acid was added, and the reaction mixture was heated for 5 days. After work-up, a brown solid soluble in common organic solvents such as chloroform, dichloromethane, or acetone and insoluble in nonpolar solvents such as hexane or diethyl ether was obtained. The functionalized and thus solubilized CNTs were also found to be stable in solution as no precipitation was observed upon standing.

Using this type of chemistry, a large number of pyrrolidine rings fused to the carbon–carbon bonds of CNTs are produced. It is this covalent attachment of a high number of functionalities that renders functionalized CNTs soluble. Of course, in order to achieve such a high degree of solubilization, the functional groups present in the starting materials have to be carefully designed. This explains the reason for choosing N-substituted glycines, characterized by the presence of solubilizing chains, such as oligoethylene glycol moieties (Scheme 3).

In order to calculate the number of pyrrolidine rings attached, a chromophore was chosen for quantitative UV–vis spectroscopy analysis. Therefore, pyrene aldehyde was allowed to react in the 1,3-dipolar azomethine ylide cycloaddition and by measuring the electronic absorption spectrum of the functionalized material, the presence of added pyrene groups were identified. Thus, one pyrene and
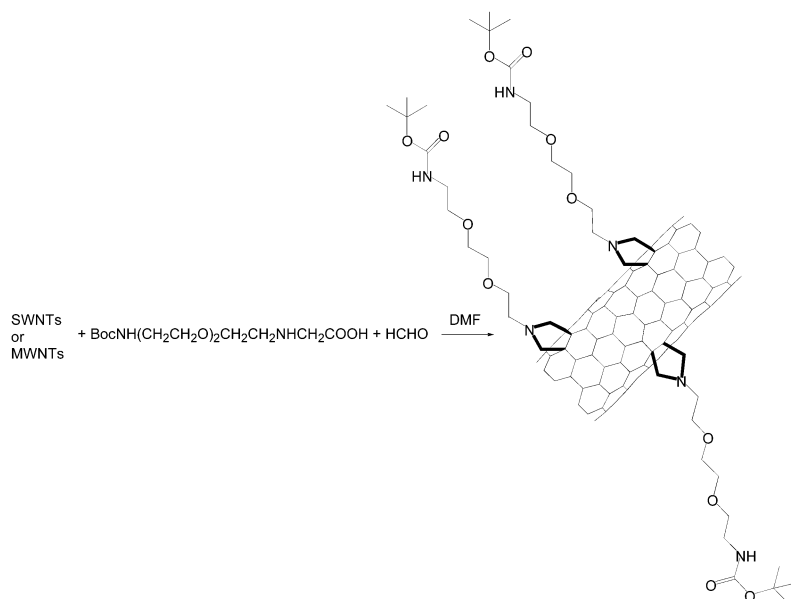
Scheme 3

therefore one pyrrolidine group (e.g., calculated by measuring the concentration of pyrene in the sample) corresponding to approximately 95 carbon atoms of SWNT was counted. By simply correlating the number of carbon atoms that form the smallest cylindrical unit of a nanotube, this is a remarkably high number of functionalities that have been covalently attached onto the surface of CNTs.

Importantly, this solubilization aids in purifying CNTs from insoluble metal nanoparticles and other carbon materials present in pristine CNTs (Fig. 3) [53]. Thus, with the following three-step procedure, purification of CNTs can be achieved: (a) organic functionalization of pristine nanotubes, (b) purification of the soluble adducts, and (c) recovery of the starting material by thermal detachment of the functional groups. The combination of these steps led to a high-purity material.
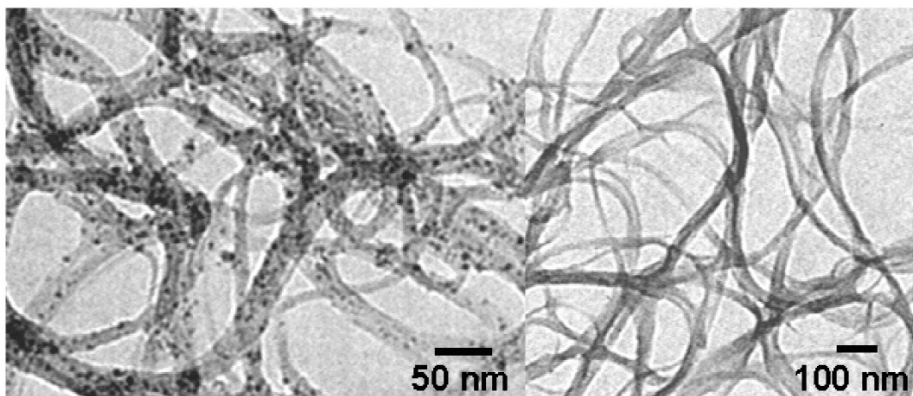

Fig. 3 TEM micrographs of pristine (left) and purified (right) nanotubes.

The first step is based on chemical modification by 1,3-dipolar cycloaddition onto the surface of nanotubes. This chemical route resulted in solubilization of the functionalized nanotubes, leaving the metal particles insoluble in the solvent used (DMF). Yet, amorphous carbon was still present since it is soluble in the reaction medium. To further purify the functionalized nanotubes, a process consisting of

dissolution and slow precipitation by using a combination of chloroform/diethyl ether mixtures, was employed. The purified material was treated thermally at temperatures reaching 350 °C under inert atmosphere. After this procedure, a weight loss of about 30 % of material was observed and was attributed to the removal of functional groups from the CNT surface. The resulting solid was annealed at 900 °C and found to be insoluble in any solvent, while TEM images showed that CNTs were recovered and most importantly were found to be free from impurities.

A two-step reaction based on the 1,3-dipolar cycloaddition of azomethine ylides was recently applied to obtain water-soluble functionalized nanotubes (Schemes 3 and 4) [54]. Thus, when N-substituted amino acid and paraformaldeyde were added to a suspension of CNTs (either single-walled or multi-walled), properly functionalized nanotubes were isolated, whereas upon treatment with gaseous hydrochloric acid, the free ammonium salt on the added *N*-alkyl chain of the pyrrolidine was released and, thus, water-soluble functionalized nanotubes were obtained. Furthermore, the free amino groups of the latter were derivatized with N-protected glycine amino acid [44], and a series of other amino acids and bioactive peptides were also attached [47,48]. In such a way, water-soluble functionalized nanotubes have been obtained and served as intermediate synthons to covalently attach peptides for future biological studies.
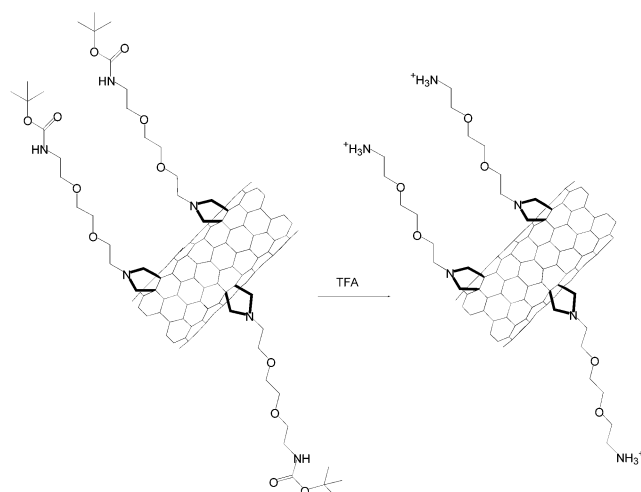
Scheme 4

Another central aspect of nanotube chemistry, which yet awaits exploration, is its function and performance in donor–acceptor ensembles. Toward this direction, the covalent linking of electron donors, such as ferrocene, onto the network of CNTs was pursued with the aim of potential use in photovoltaics. Indeed, utilizing ferrocene-modified glycine and paraformaldehyde, soluble CNTs decorated with many ferrocene (Fc) units all around their skeleton were obtained (Scheme 5) [45].

Electron transfer from the ferrocene units to CNTs occurs upon photoexcitation, whereas the slow kinetics of charge recombination between the two components holds promise for future developments of such CNT-based ensembles in solar-energy conversion. These Fc-CNT nanohybrid materials can also be used as chemical sensors and biosensors for the selective recognition of anions. Selective recognition of anions is a relevant argument in light of biological and environmental interests. The clustering of a large number of Fc units around the CNT core together with the increased solubility enhance the supramolecular interaction with $H_2PO_4^-$ anions in organic solutions [46]. Moreover, the co-immobilization of glucose oxidase and such Fc-functionalized CNTs, as suitable redox mediator, within a polypyrrole film adsorbed onto a glassy carbon electrode surface was utilized for the construction of a glucose amperometric biosensor [51].
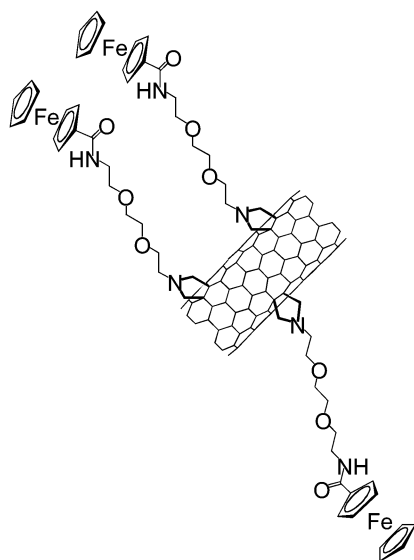
Scheme 5

The confirmation and elemental characterization of all the functionalized nanotubes was accomplished by complementary analytical techniques such as infrared (IR), proton nuclear magnetic resonance (^{1}H NMR), and raman spectroscopy. However, proton signals appear to be broad as a result of the statistical distribution of the addends on the CNT surface. Furthermore, interactions between the protons of the addends and the π-system of CNTs as well as the restricted mobility of CNTs in solution due to their large size contribute to line-broadened signals. On the other hand, raman spectroscopy is an extremely useful tool for characterizing CNTs, as they exhibit two main characteristic absorptions: the diameter-dependent radial breathing mode (RBM) at 250 cm^{-1} and the higher-frequency tangential mode at 1580 cm^{-1}, respectively, while in addition, functionalized CNTs show a third mode at 1295 cm^{-1}, the so-called disorder or sp^3 mode and its relative intensity seems to correspond to the degree of disruption (functionalization) of the CNT framework. Of course, the use of the above spectroscopies alone does not confirm that the pyrrolidine tails are appended onto the sidewalls of CNTs. The latter is confirmed by state-of-the-art microscopy techniques such as TEM, scanning electron microscopy (SEM), and atomic force microscopy (AFM), which unambiguously revealed the presence of CNTs on the derivatized samples. However, the presence of the added functional groups is not clear from TEM images, careful analysis and comparison of these images with the ones derived from pristine nanotubes reveal important differences that can be attributed to the modification of the nanotube surface. Thus, functionalized CNTs are associated in thinner bundles or ropes as compared to the pristine CNTs. Eventually, the functionalized and, thus, solubilized CNTs are found to be even purer in comparison with the pristine material, which contains large amounts of amorphous carbon and metal nanoparticles.

Research on CNTs has opened up new avenues in materials science such that great opportunities for applications in nanotechnology are offered. A plethora of novel materials such as the above-mentioned organic functionalized nanotube derivatives or nanocomposites can be produced with a wide variety of properties related to the attached functional group. Nevertheless, with further developments in fabrication and manipulation, new sections of nanotechnology can be based on the advances made for CNTs.

ACKNOWLEDGMENTS

REFERENCES

1. J.-M. Lehn. *Proc. Natl. Acad. Sci. USA* **99**, 4763 (2002).
2. A. M. Cassel, C. Lee Asplund, J. M. Tour. *Angew. Chem., Int. Ed.* **38**, 2403 (1999).
3. P. D. W. Boyd, M. C. Hodgson, C. E. F. Rickard, A. G. Oliver, L. Chaker, P. J. Brothers, R. D. Bolskar, F. S. Tham, C. A. Reed. *J. Am. Chem. Soc.* **121**, 10487 (1999).
4. V. Georgakilas, F. Pellarini, M. Prato, D. M. Guldi, M. Melle-Franco, F. Zerbetto. *Proc. Natl. Acad. Sci. USA* **99**, 5075 (2002).
5. S. Xiao, Y. Li, H. Fang, H. Li, H. Liu, Z. Shi, L. Jiang, D. Zhu. *Org. Lett.* **4**, 3063 (2002).
6. D. Sun, F. S. Tham, C. A. Reed, P. D. W. Boyd. *Proc. Natl. Acad. Sci. USA* **99**, 5088 (2002).
7. L. Sanchez, M. T. Rispens, J. C. Hummelen. *Angew. Chem., Int. Ed.* **41**, 832 (2002).
8. M. Kimura, Y. Saito, K. Ohta, K. Hanabusa, H. Shirai, N. Kobayashi. *J. Am. Chem. Soc.* **124**, 5274 (2002).
9. S. H. Kang, H. Ma, M.-S. Kang, K.-S. Kim, A. K.-Y. Jen, M. Hadi Zareie, M. Sarikaya. *Angew. Chem., Int. Ed.* **43**, 1512 (2004).
10. N. Katsonis, A. Marchenko, D. Fichou. *Adv. Mater.* **16**, 309 (2004).
11. M. Maggini, G. Scorrano, M. Prato. *J. Am. Chem. Soc.* **115**, 9798 (1993).
12. M. Prato and M. Maggini. *Acc. Chem. Res.* **31**, 519 (1998).
13. N. Tagmatarchis and M. Prato. *Synlett* 768 (2003).
14. N. Tagmatarchis and M. Prato. In *Structure and Bonding*, K. Prassides (Ed.), Chap. 1, pp. 1–39, Springer-Verlag, Heidelberg (2004).
15. H. Imahori and Y. Sakata. *Eur. J. Org. Chem.* 2445 (1999).
16. D. M. Guldi. *Chem. Commun.* 321 (2000).
17. D. M. Guldi and M. Prato. *Acc. Chem. Res.* **33**, 695 (2000).
18. D. Gust, T. A. Moore, A. L. Moore. *Acc. Chem. Res.* **34**, 40 *(*2001).
19. D. M. Guldi. *Chem. Soc. Rev.* **31**, 22 (2002).
20. H. Imahori, N. Tkachenko, V. Vehmanen, K. Tamaki, H. Lemmetyinen, Y. Sakata, S. Fukuzumi. *J. Phys. Chem. A* **105**, 1750 (2001).
21. D. M. Guldi, C. Luo, M. Prato, A. Troisi, F. Zerbetto, M. Scheloske, E. Dietel, W. Bauer, A. Hirsch. *J. Am. Chem. Soc.* **123**, 9166 (2001).
22. R. Williams, M. Koeberg, J. Lawson, Y.-Z. An, Y. Rubin, M. Paddon-Row, J. W. Verhoeven. *J. Org. Chem.* **61**, 5055 (1996).
23. J. Bourgeois, F. Diederich, L. Echegoyen, J.-F. Nierengarten. *Helv. Chim. Acta* **81**, 1835 (1998).
24. A. M. Cassell, C. L. Asplund, J. M. Tour. *Angew. Chem., Int. Ed. Engl.* **38**, 2403 (1999).
25. H. Murakami, M. Shirakusa, T. Sagara, N. Nakashima. *Chem. Lett.* 815 (1999).
26. D. M. Guldi, M. Maggini, S. Mondini, F. Guerin, J. H. Fendler. *Langmuir* **16**, 1311 (2000).
27. S. J. Tans, A. R. M. Verschueren, C. Dekker. *Nature* **393**, 49 (1998).
28. H. Dai, E. W. Wong, C. M. Lieber. *Science* **272**, 523 (1996).
29. B. I. Yakobson and R. E. Smalley. *Am. Sci.* **85**, 324 (1997).
30. P. M. Ajayan. *Chem. Rev.* **99**, 1787 (1999).
31. D. Antonov and A. T. Johnson. *Phys. Rev. Lett.* **83**, 3274 (1999).
32. Z. Yao, H. W. Ch. Postma, L. Balents, C. Dekker. *Nature* **402**, 273 (1999).
33. C. Zhou, J. Kong, E. Yenilmez, H. Dai. *Science* **290**, 155 (2000).

34. H. W. Ch. Postma, T. Teepen, Z. Yao, M. Grifoni, C. Dekker. *Science* **293**, 76 (2001).
35. A. Bachtold, P. Hadley, T. Nakanishi, C. Dekker. *Science* **294**, 1317 (2001).
36. A. Hirsch. *Angew. Chem., Int. Ed.* **41**, 1853 (2002).
37. J. L. Bahr and M. Tour. *J. Mater. Chem.* **12**, 1952 (2002).
38. S. Niyogi, M. A. Hamon, H. Hu, B. Zhao, P. Bhomwik, R. Sen, M. E. Itkis, R. C. Haddon. *Acc. Chem. Res.* **35**, 1105 (2002).
39. Y.-P. Sun, K. Fu, Y. Lin, W. Huang. *Acc. Chem. Res.* **35**, 1096 (2002).
40. S. Banerjee, M. G. C. Kahn, S. S. Wang. *Chem. Eur. J.* **9**, 1898 (2003).
41. D. Tasis, N. Tagmatarchis, V. Georgakilas, M. Prato. *Chem. Eur. J.* **9**, 4000 (2003).
42. C. A. Dyke and J. M. Tour. *Chem. Eur. J.* **10**, 812 (2004).
43. V. Georgakilas, K. Kordatos, M. Prato, D. M. Guldi, M. Holzinger, A. Hirsch. *J. Am. Chem. Soc.* **24**, 760 (2002).
44. V. Georgakilas, N. Tagmatarchis, D. Pantarotto, A. Bianco, J.-P. Briand, M. Prato. *Chem. Commun.* 3050 (2002).
45. D. M. Guldi, M. Marcaccio, D. Paolucci, F. Paolucci, N. Tagmatarchis, D. Tasis, E. Vasquez, M. Prato. *Angew. Chem., Int. Ed.* **42**, 4206 (2003).
46. A. Callegari, M. Marcaccio, D. Paolucci, F. Paolucci, N. Tagmatarchis, D. Tasis, E. Vazquez, M. Prato. *Chem. Commun.* 2576 (2003).
47. D. Pantarotto, C. D. Partidos, J. Hoebeke, F. Brown, E. Kramer, J.-P. Briand, S. Muller, M. Prato, A. Bianco. *Chem. Biol.* **10**, 961 (2003).
48. D. Pantarotto, C. D. Partidos, R. Graff, J. Hoebeke, J.-P. Briand, M. Prato, A. Bianco. *J. Am. Chem. Soc.* **125**, 6160 (2003).
49. A. Bianco and M. Prato. *Adv. Mater.* **20**, 1765 (2003).
50. N. Tagmatarchis and M. Prato. *J. Mater. Chem.* **14**, 437 (2004).
51. A. Callegari, S. Cosnier, M. Marcaccio, D. Paolucci, F. Paolucci, V. Georgakilas, N. Tagmatarchis, E. Vasquez, M. Prato. *J. Mater. Chem.* **14**, 807 (2004).
52. D. Pantarotto, J.-P. Briand, M. Prato, A. Bianco. *Chem. Commun.* 16 (2004).
53. V. Georgakilas, D. Voulgaris, E. Vazquez, M. Prato, D. M. Guldi, A. Kukovecz, H. Kuzmany. *J. Am. Chem. Soc.* **124**, 14318 (2002).